scientific reports

Check for updates

OPEN

Lipidomics of prolonged labor duration in African American birthing people

Nicole S. Carlson✉, Chih-Yu Chen, Zhenxin Hou, Xueyun Liu-Gulbin, Jessica Alvarez, Anne L. Dunlop & Kristal Maner-Smith

Labor dystocia, a leading indication for cesarean delivery, disproportionately affects African American women, yet its metabolic underpinnings remain poorly understood. The objective of this study was to characterize prenatal serum lipidomic signatures associated with term labor dystocia in African American women. Untargeted lipidomics was performed on serum collected at early (8–14 weeks) and late-pregnancy (24–30 weeks) from 43 labor dystocia cases matched to 43 rapid labor controls on parity, BMI, age and mode of labor onset. Analyses included PLS-DA, weighted lipid co-expression network analysis, community structure analysis, and longitudinal difference-of-difference modeling. Labor dystocia was characterized by reduced circulating LPC, ceramide, and sphingomyelin in early pregnancy alongside elevated polyunsaturated PE and PI species. Late pregnancy was marked by progressive accumulation of saturated and oleic acid-containing triglycerides. Network analysis revealed reorganization of inter-module lipid relationships with loss of negative regulatory correlations in dystocia. Integrating longitudinal lipid trajectories yielded superior predictive performance (AUC 0.979) compared to single time-point models. Labor dystocia is preceded in pregnancy by a disrupted circulating lipid signature, providing preliminary leads for future research to support early risk stratification and understanding of the mechanisms underlying prolonged labor.

Keywords Pregnancy, Labor duration, Lipid, Parturition

Unplanned cesarean birth is a principal driver of maternal morbidity and mortality[1]. When pregnancy ends in cesarean delivery, there is an increased risk for postpartum infection, hemorrhage, and other surgical complications, all of which are associated with higher rates of morbidity or mortality[2]. A common clinical indication for cesarean birth is labor dystocia, defined as the abnormally slow progression of active phase labor, a dynamic time during labor's first stage when the ripened cervix dilates from around 5 to 10 cm under the influence of strong, repetitive uterine contractions[3,4].

Elevated maternal body mass index (BMI) is a well-known predictor of labor dystocia, which in turn increases the risk for cesarean birth in analyses controlling for the influence of parity, pregnancy complications, and system characteristics[5–8]. A theoretical mechanism of slow labor progress in the presence of obesity is lipotoxicity, whereby excess free fatty acids from the diet are used for cellular energy and storage in non-adipose tissue deposits, causing widespread cellular damage and dysfunction[9–11]. In studies by this group[12,13] and others[9,14], support for this theoretical mechanism of labor dystocia includes the observation of ectopic fat deposits in the uterine muscle tissue from women with obesity, resulting in a reduction of lean muscle mass in that organ[9], and findings using untargeted metabolomics that perturbations of fatty acid activation predicted longer durations of labor during induction in humans[12] and during spontaneous labor in mice[14].

Lipids are responsible for a range of functions in the human body, including storage of energy reserves, formation of cell and plasma membranes, signal transduction, chemical messaging, and regulation of proteins[15]. The lipidome, defined as the full complement of lipids in an organism, includes eight different lipid categories, each with multiple sub-groups, which are interconnected via complex pathways and networks to exert their physiological effects. Lipidomics, by which the lipidome is interrogated using a combination of mass spectrometry and advanced computation, is like other -omics methodologies in offering investigators opportunities for discovery of physiologic processes underlying disease processes. Given their chemical properties, lipids are difficult to detect at sufficient granularity in a metabolomics laboratory process[16–20]; thus, lipidomics offers the potential to better describe lipid-dominated processes[15,21].

Emory University, 1520 Clifton Road NE, Atlanta, GA 30322, USA. ✉email: Nicole.carlson@emory.edu

In this group's previous metabolomics study, labor dystocia was differentiated by linoleate metabolism pathway enrichment, in addition to fatty acid activation and metabolism[13]. That metabolomics investigation corroborated a previous study using a rat model of obesity, in which investigators noted decreased plasma and uterine levels of omega-3 PUFAs in rats fed a high cholesterol/high fat diet compared to those taking normal diet during pregnancy, causing decreases in uterine contraction strength and coordination at term[22,23]. Therefore, in the current investigation we used not only untargeted lipidomics, but also targeted lipidomics to characterize and quantify polyunsaturated fatty acid (PUFA) metabolism, including levels of linoleate and arachidonic acids. From a retrospective cohort of healthy African–American women who labored at term with the same groups of clinicians, we conducted a case–control study to identify both untargeted lipidomic and targeted oxylipin lipidomic profiles in serum collected during pregnancy associated with a labor dystocia phenotype. We hypothesized that women who showed evidence of labor dystocia would have distinct pregnancy lipidomic profiles with specific reductions in circulating PUFAs, compared to similar women who showed no evidence of labor dystocia.

Results

A total of 173 parent study participants met inclusion criteria (term gestation and vertex fetus, completed first stage labor or had a cesarean for the primary indication of labor dystocia) for this study. For the case–control sample, participants were selected for the labor dystocia (n = 43) or rapid labor comparison (n = 43) groups with matching for parity, mode of labor onset, maternal body mass index (BMI), and maternal age. Participants in these groups were therefore similar in parity (46.5% nulliparous), age (median 25 years, IQR ± 7), self-identified race (100% African–American), initial prenatal visit body mass index (BMI, median 26.8 kg/m^2, IQR ± 11.9), and median BMI at the time of admission for delivery (32.0, IQR ± 12.3) (Table 1). Although infrequent, the development of gestational diabetes occurred in more labor dystocia cases (7.0%) than comparisons (0%). During labor, there was no difference between groups in the gestational age at labor admission (39.4 weeks, IQR ± 1.4), or mode of labor onset (39.5% had labor induction). Among those with labor induction (n = 34), there was no difference between groups in their cervical dilation at hospital admission (1.0 cm, IQR ± 2.0). However, labor dystocia cases had significantly longer active phase labor durations (686 ± 672 min vs. 75 ± 101 min in the comparison group), with more frequent use of epidural analgesia (97.7% vs. 39.5%), amniotomy (76.7% vs. 37.2%), cesarean delivery (18.6% vs. 4.7%) and complications linked to longer labor duration like intrapartum infection diagnosis (21.4% vs. 0%) and postpartum hemorrhage (11.6% vs. 7.0%). Included among labor dystocia cases were three participants who had cesarean for labor dystocia prior to reaching the end of active phase labor. In all three of these participants, the duration of active phase labor prior to cesarean surpassed the highest tertile of active phase labor duration in the overall cohort (mean active labor duration in these three participants prior to cesarean = 2161 min). Thus, our matching strategy for the case/control sample was successful in creating two groups of participants who were similar in all pregnancy risk factors for labor dystocia (maternal age, parity, BMI) and known intrapartum risk factors for longer labor (induced labor), yet labor dystocia cases had active phase labors which lasted nearly 9 times longer than comparison cases, or had cesarean birth for active phase arrest despite laboring for an average of 36 h.

Lipidomic analysis was completed on serum collected from participants in both early pregnancy (visit 1, 8–14 weeks' gestation) and late pregnancy (visit 2, 24–30 weeks' gestation). A comprehensive lipidomics analysis was conducted using both targeted and untargeted approaches to have a broad coverage of the serum lipidome. The targeted lipidomic method (multiple reaction monitoring, MRM) yielded a total of 29 oxylipins, endocannabinoids, and non-esterified fatty acids (NEFA) in the samples, but no long-chain PUFAs (Tables S6 and S9), after data filtering criteria were met. The untargeted lipidomic approach employed data-dependent acquisition (DDA) method of high-resolution accurate-mass and ddMS2 data acquisition using UPLC orbitrap MS/MS, and resulted in 570 annotated lipids (validated lipids are listed in Table S3) (Fig. 1A).

Lipidome changes associated with labor dystocia phenotype

First, we compared labor dystocia cases and comparison sera for key lipid differentiators. For this analysis, we focused on visit 1 sera, and secondarily on visit 2 serum lipids. Among the labor dystocia case/control groups created for this study, a total of four participants did not have a visit 1 sample and were thus dropped from this analysis, leaving n = 82 participants (Fig. 1B).

Among the 570 lipids identified with the untargeted approach and after normalization, a total of 17 lipid classes were measured among all sera for the 82 participants from the labor dystocia and comparison groups, with the first and second in net abundance being triacylglycerols (TG) and phosphatidylcholine (PC) species, respectively (Fig. S2B). As depicted in Fig. 1C, univariate results showed that in early pregnancy (at visit 1), the labor dystocia group (Dys) had significantly lower levels of lysophosphatidylcholine (LPC), cholesteryl ester (ChE), sphingomyelin (SM) and ceramide (Cer) compared to the rapid labor comparison group (Con). PC levels were similar between groups, resulting in a significantly reduced LPC/PC ratio in Dys group ($p = 0.0001$). Additionally, phosphatidylethanolamine (PE) levels were slightly decreased in Dys group, contributing to a higher ratio of PC/PE ($p = 0.0038$). Although levels of diacylglycerols (DG) and TG were comparable between groups, the DG/TG ratio tended to be lower in Dys than in Con group. During late pregnancy (visit 2), sera from the labor dystocia group had significantly higher serum TG levels than the control group, leading to a lower ratio of DG/TG ($p = 0.089$), a trend that was also observed in early pregnancy. We saw no significant differences between groups for other lipid classes at visit 2, except acylcarnitine (AcCa), which was significantly decreased in labor dystocia group compared to the control group (Fig. S3A).

To identify lipid metrics most informative for distinguishing cases of labor dystocia, we employed sparse partial least-squares discriminant analysis (sPLS-DA) as an exploratory classification tool. In early pregnancy (visit 1), based on 18 key lipid metrics selected by the model, we found that the control and dystocia groups

	Total sample (N = 86)	Labor dystocia case (n = 43)	Comparison case (n = 43)	*p*-value[a, b]
Maternal demographic				
Race: African-American (n, %)	86 (100)	43 (100)	43 (100)	1.0
Insurance: Medicaid (n, %)	61 (70.9)	31(72.1)	30 (69.8)	0.11
Maternal age (years, median ± IQR)	25.0 (7)	24.0 (7)	25.0 (7)	0.19
Pregnancy characteristics				
First prenatal BMI (kg/m^2, median ± IQR)	26.8 (11.9)	28.5 (16.8)	25.6 (11.9)	0.29
Delivery BMI (kg/m^2,median ± IQR)[c]	32.0 (12.3)	33.9 (13.2)	31.1 (11.9)	0.10
Nulliparous (n, %)	40 (46.5)	20 (46.5)	20 (46.5)	1.0
Gestational diabetes (n, %)[d]	3 (3.6)	3 (7.0%)	0	**0.04**
Labor characteristics				
Gestational age at labor admission (weeks, median ± IQR)	39.4 (1.4)	39.3 (1.7)	39.4 (1.5)	0.39
Labor induction (n, %)	34 (39.5)	17 (39.5)	17 (39.5)	1.0
Cervical dilation at IOL onset (cm, median, IQR)[e]	1 (2.0)	1 (2.5)	1 (1.0)	0.59
Infection during labor (n, %)[f]	9 (10.8)	9 (21.4)	0	**< 0.001**
Spontaneous membrane rupture (n, %)	37 (43.0)	10 (23.3)	27 (62.8)	**< 0.001**
Epidural in labor (n, %)	59 (68.6)	42 (97.7)	17 (39.5)	**< 0.001**
Active labor duration (minutes, median ± IQR)[g]	288.0 (610)	686 (672)	75 (101)	**< 0.001**
Labor Outcomes				
Type of Delivery (n, %)				
Vaginal	76 (88.4)	35 (81.4)	41 (95.3)	0.37
Cesarean Section	10 (11.6)	8 (18.6)	2 (4.7)	
Postpartum hemorrhage (> 500 ml, n %)	8 (9.3)	5 (11.6)	3 (7.0)	0.47
Newborn sex (n, %)				
Male	42 (48.8)	23 (53.5)	19 (44.2)	0.39
Female	44 (51.2)	20 (46.5)	24 (55.8)	
Newborn NICU admission (n, %) [h]	4 (4.7)	3 (7.0)	1 (2.4)	0.31
Neonatal birthweight (grams, mean ± SD)	3192.5 (411.1)	3266.2 (418.9)	3118.9 (394.2)	0.97

Table 1. Maternal, pregnancy, and labor characteristics/outcomes in case–control labor dystocia matchedsample (N = 86). [a]*p*-value for comparison between labor dystocia cases and comparison group. Likelihood ratio significance testing for categorical variables and t- test or Mann–Whitney U test used for continuous variables. *p*-value < 0.05 shown in bold font. [b] Median and Interquartile Range (IQR) shown for non-normally distributed continuous variables; Mean and Standard Deviation (SD) shown for normally-distributed variables (Shapiro Wilk test significant < 0.05). [c] Delivery BMI missing for 1 participant in the dystocia group and 2 in the comparison group. [d] Gestational diabetes information missing for 3 in comparison group. [e] Cervical dilatation reported at hospital admission per clinical examination for participants who were induced (n = 34). [f] Missing information on diagnosis of infection during labor on 1 in the dystocia and 2 in the comparison group. [g]Active phase labor total duration calculated as the time to complete cervical dilation (10 cm) for participants with either induced (4–10 cm dilation) or spontaneous labor onset (5–10 cm), based on clinician cervical examination. Missing for three members of the labor dystocia group who had cesarean delivery for indication of labor dystocia. [h]NICU admission information missing for 1 in the comparison group.

were distinguished with a classification error rate of 0.284 (71.6% accuracy)(Fig. 2B). The unbiased nested cross-validation (CV) performance was lower, with an AUC of 0.728 (95% confidence interval (CI): 0.577–0.986; Fig. 2C). Among lipid features selected to differentiate labor dystocia, 50% were polyunsaturated phospholipids, with increased levels in the dystocia group (Fig. 2D). Notably, PE (42:9) emerged as a potential individual discriminator, yielding an AUROC of 0.764 and a nested-CV AUC of 0.783 (95% CI 0.605–0.937; Fig. S4B), and was present at higher levels in the dystocia group (Fig. 2D). During late pregnancy (visit 2), a total of 79 lipids significantly altered between the groups were used for sPLS-DA with a feature selection method. Model performance and classification error for visit 2 lipids, compared to the models using visit 1 lipids, was slightly lower. At visit 2, 16 lipids were selected in the model, yielding an AUROC of 0.888 (67.1% accuracy) and a nested-CV AUC of 0.658 (95% CI 0.451–0.798). Most of the selected lipids contributing to the group separation at visit 2 were TG containing palmitic acid (C16:0), oleic acid (C18:1) or linoleic acid (C18:2), all of which were elevated in the labor dystocia group (Fig. S5G).

In summary, PLS-DA analysis distinguished labor dystocia from rapid labor groups at both visits, with early pregnancy performing better than late pregnancy. Key early pregnancy features differentiating term labor dystocia included reduced LPC, cholesteryl ester, and ceramide, with elevated polyunsaturated phospholipids; late pregnancy discrimination was driven primarily by elevated saturated and monounsaturated TG species in the dystocia group.

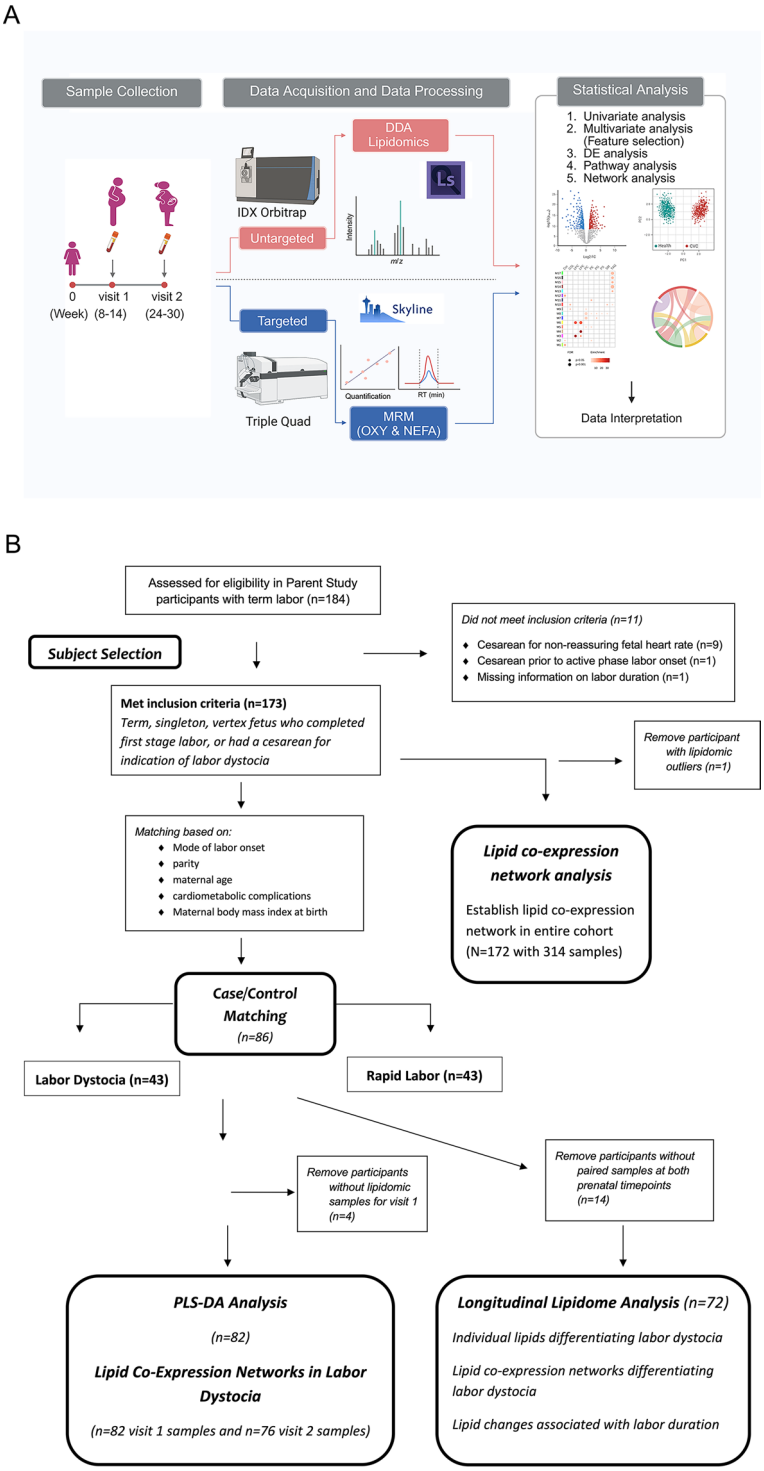

Fig. 1. Lipidome analysis of pregnancy African American women. (**A**) Schematic experimental design. Blood samples were collected from pregnant African American women at visit 1 and visit 2. Lipid analysis was conducted using mass spectrometry-based techniques, including DDA and MRM, followed by statistical analysis. (**B**) Subject selection flowsheet. (**C**) Boxplots of individual subjects in both Comparison and Dystocia groups, displaying the median and interquartile range for each lipid class. Lipid class values were calculated as the sum of all lipids within the same class, using normalized peak areas relative to internal standards. Student's t-tests were used to assess statistically significant differences between the means of the two groups ($p < 0.05$). Subject numbers at visit 1: 41 dystocia and 41 comparison.

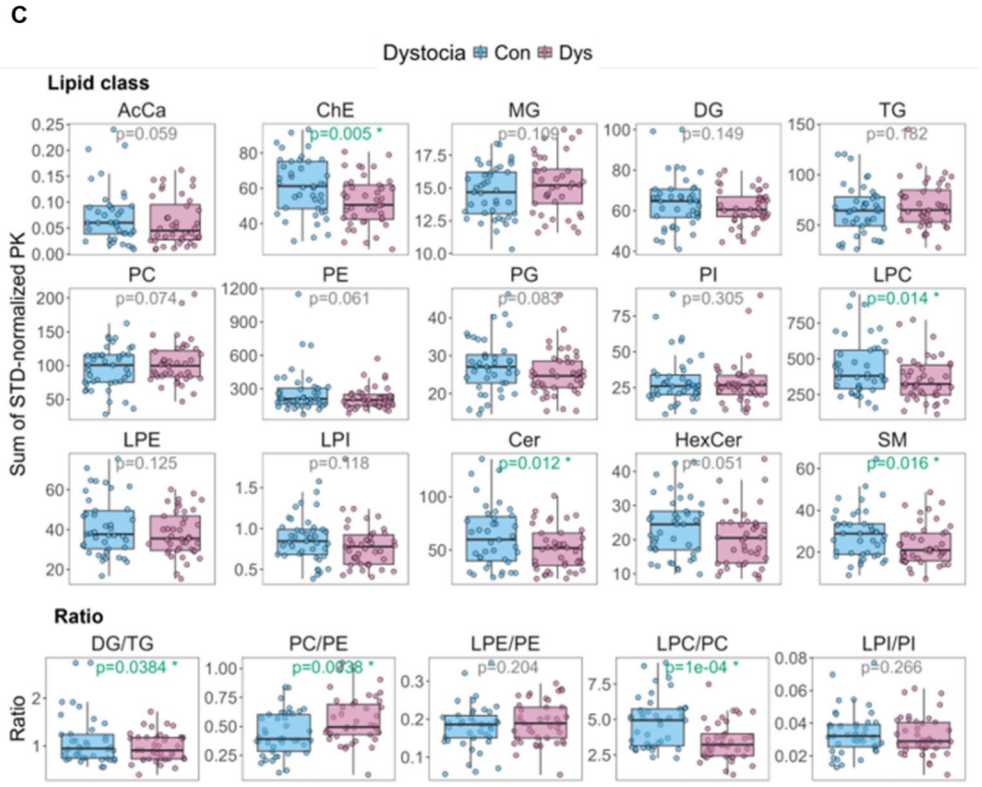

Fig. 1. (continued)

Network analysis reveals differential lipid modules between groups

For the next part of our analysis, we analyzed lipid co-expression networks to detect if any lipid modules, or clusters of structurally related lipid species that co-vary in both abundance and functionality, were associated with the labor dystocia phenotype. For this analysis, we first performed WGCNA using lipidomics data from the entire cohort, combining visit 1 and visit 2 samples, to ensure robust module detection (172 participants, 314 samples) (Fig. 1B). After characterizing the lipid modules active in the entire cohort, we then compared lipid modules between the matched labor dystocia cases/control sera. Module eigengenes were derived and examined for their associations with clinical traits separately at each visit, and the comparison of lipid modules between two groups, allowing us to assess how module-trait relationships differed between early (visit 1) and late (visit 2) pregnancy (Visit 1: Con n = 41, Dys n = 41; Visit 2: Con n = 37, Dys n = 39, including participants who attended only one visit). This analysis yielded a network with 15 lipid modules, each ranging in size from 12 to 138 lipids, after excluding 2 outliers. Detailed information, including method, module membership (MM), module eigengene values (MEs), *p* values, and other relevant data, is presented in Figs. S6, 7, Table S10, and the supplementary materials.

In early pregnancy, five lipid modules (M6, M9, M10, M13, and M14) were significantly associated with labor dystocia (Fig. 3). Overall, the M6 and M14 modules exhibited higher MEs in the dystocia group, while M9, M10, M13 modules showed lower MEs compared to the control group (Fig. 3B). The M6 module was predominantly enriched in PE (Fig. 3A), particularly those containing polyunsaturated fatty acids (PUFA). Notably, the polyunsaturated PE in the M6 module featured mainly arachidonic acid (C20:4, AA) and docosahexaenoic acid (C22:6, DHA) fatty acyl chains, and showed a trend toward increased levels in Dys group (Fig. 4A). Another important lipid module differentiating labor dystocia cases in early pregnancy was the M9 module, enriched in long chain or very long chain Cer and hexosylceramide (HexCer), which showed significantly reduced levels of total C22 and C24 Cer in Dys than Con group (Fig. 4B). Modules M10 and M13, which were both enriched in LPC in positive and negative modes respectively (Fig. 3A), included LPC species with chain lengths ranging from 14 to 22 carbons and desaturation levels from 0 to 6. All LPC species were consistently lower in the dystocia group than in the control group, with LPC 20:5 showing significantly decreased in both ESI modes (Fig. 4C,D). Additionally, the M14 module was enriched in phosphatidylinositol (PI) (Fig. 3A), with a general increase of the relative abundance of fatty acyl chains with various degrees of desaturation in dystocia compared to the control group. Only PI-containing omega-3 FA was significantly elevated (Fig. 4E).

During late pregnancy, the M8 module was the only module showing significantly greater MEs in dystocia compared to the control group (Fig. S8B), in which 80% of lipid species were TGs containing two saturated fatty acyl chains ($p < 0.05$) (Fig. 4F). Thus, initial lipid module analysis revealed that early pregnancy lipid modules associated with labor dystocia were characterized by elevated polyunsaturated PE (M6), reduced long-chain ceramides (M9), consistently lower LPC species (M10/M13), and increased omega-3 PI (M14), while in late pregnancy, the M8 module stood out with elevated saturated-chain triglycerides in the dystocia group.

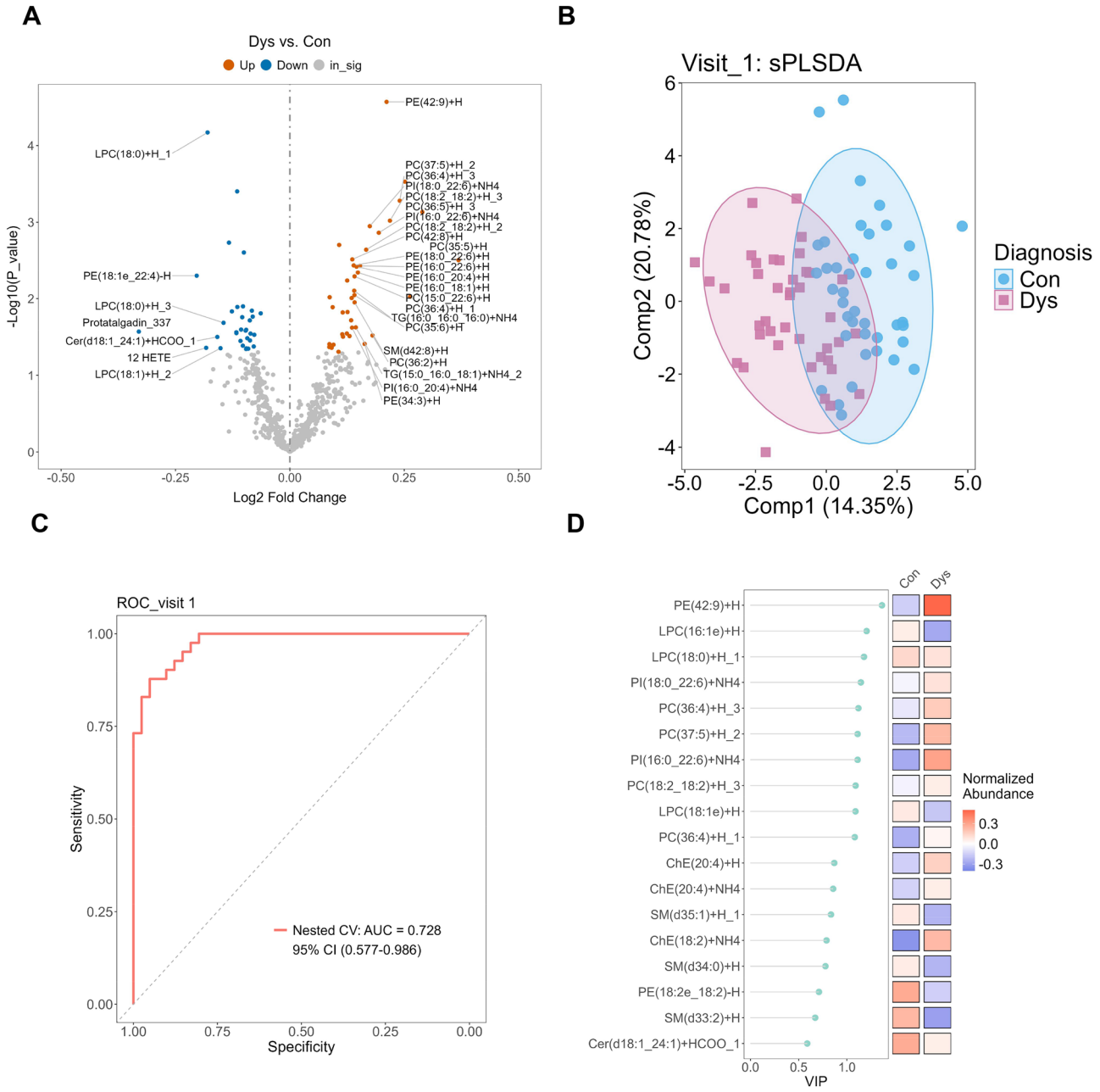

Fig. 2. Identification of differentially abundant lipid species between dystocia and comparison groups. (**A**) Volcano plot showing the $\log_2$ fold changes versus the $-\log_{10}(p\ value)$ for differential expression analysis comparing the dystocia to comparison groups (Con). Lipid species that significantly increased in abundance are shown in red, while those that significantly decreased are indicated in blue. The top thirty lipid species with the greatest absolute $\log_2$ fold changes are labelled. (**B**) Supervised PLS-DA analysis of lipidomic data after feature selection. The first two latent components (Comp 1 and Comp 2) are shown with 95% confidence ellipses surrounding each cluster core. (**C**) Receiver operating characteristic (ROC) curve and area under curve (AUC) for lipid species selected in sPLS-DA. ROC curve showing model performance with unbiased nested cross-validation (AUC = 0.728, 95% CI 0.577–0.986). The diagonal dashed line indicates no-discrimination performance. (**D**) VIP plot illustrating the average normalized values of all 18 selected features from the sPLS-DA analysis.

At a higher order of network organization beyond individual lipid modules, community structure analysis of module-module interactions revealed distinct rewiring of lipid metabolic relationships between labor dystocia and control groups at visit 1. For example, in the control group, community 1 comprised modules M1, M3, M5, M7, M9, M11, and M13, while community 2 comprised modules M2, M4, M6, M8, M10, M12, and M14. Conversely, in the labor dystocia group, TG-enriched modules M1 and M7 shifted to community 2, whereas the ether-linked PC-enriched module M2 and ether-linked PE-enriched M4 were reassigned to community

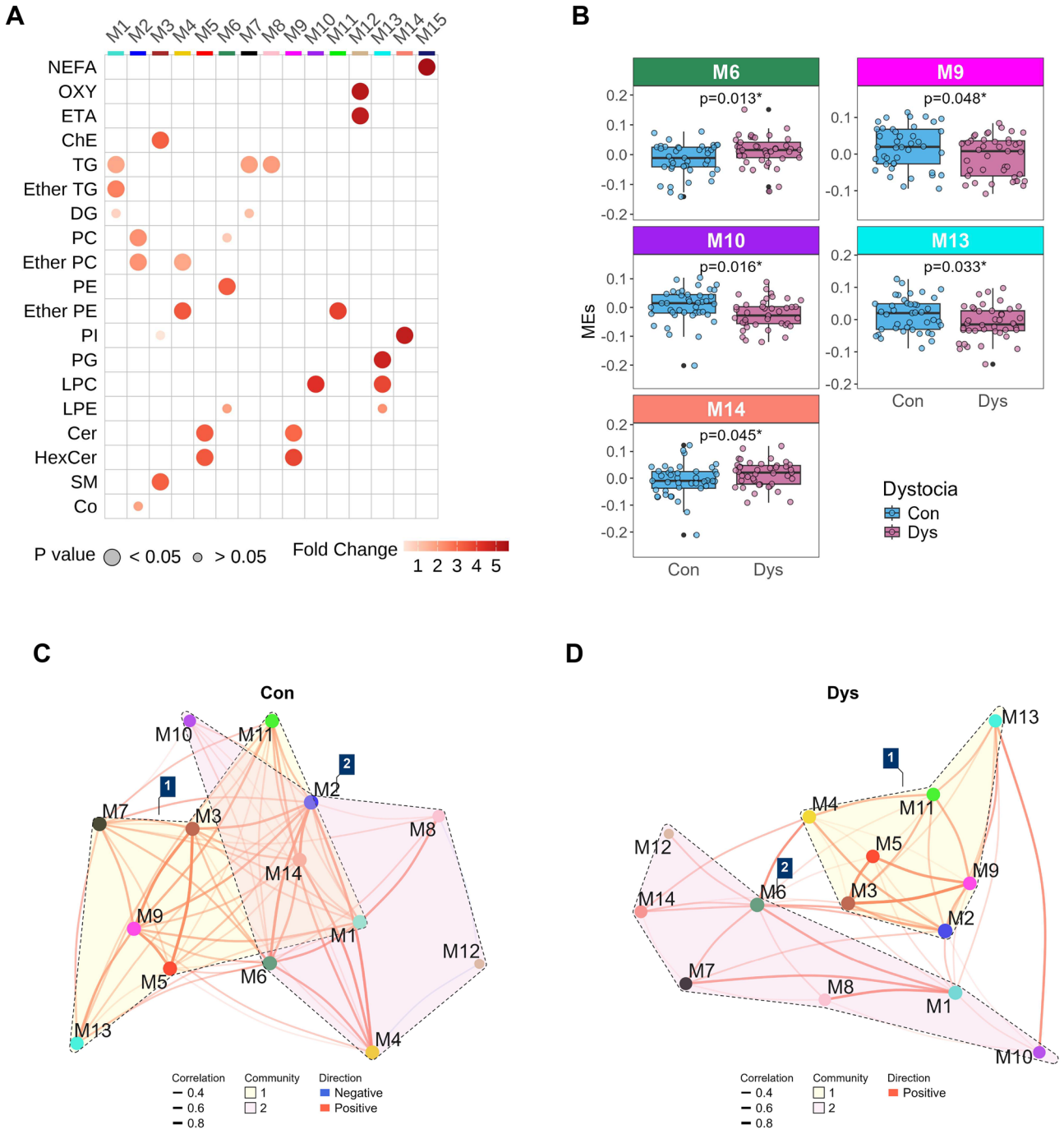

Fig. 3. Network analysis of serum lipidomics using WGCNA. (**A**) A bubble heatmap showing the lipid class enrichment in each of the 15 modules. The size of the bubble indicates the *p*-value (the larger the bubble size, the lower the *p*-value), and the color of the bubble indicates the overlap between the lipid subset and the lipid class in the background data. (logFC) of the lipid classes in each module. *p*-values were calculated using Fisher's exact test. (**B**) Boxplots showing the difference in ME values between dystocia and comparison groups at visit 1. Modules with *p*-values achieving statistical significance ($p < 0.05$) are shown here. Correlations between each module in the network analysis, shown in (**C**) for the comparison (Con) group and (**D**) for the dystocia (Dys) group. The correlation threshold was set at 0.1, with $p < 0.05$.

1. Specifically, oxylipins (OXY) and N-acylethanolamines (ETA)-enriched M12 was negatively associated with M4 in control group, an association that was not observed in dystocia group. Instead, M12 was connected to M6, suggesting a metabolic shift from ether to ester linkage in labor dystocia group. These community-level differences suggest that labor dystocia is associated with a fundamental reorganization of lipid metabolic

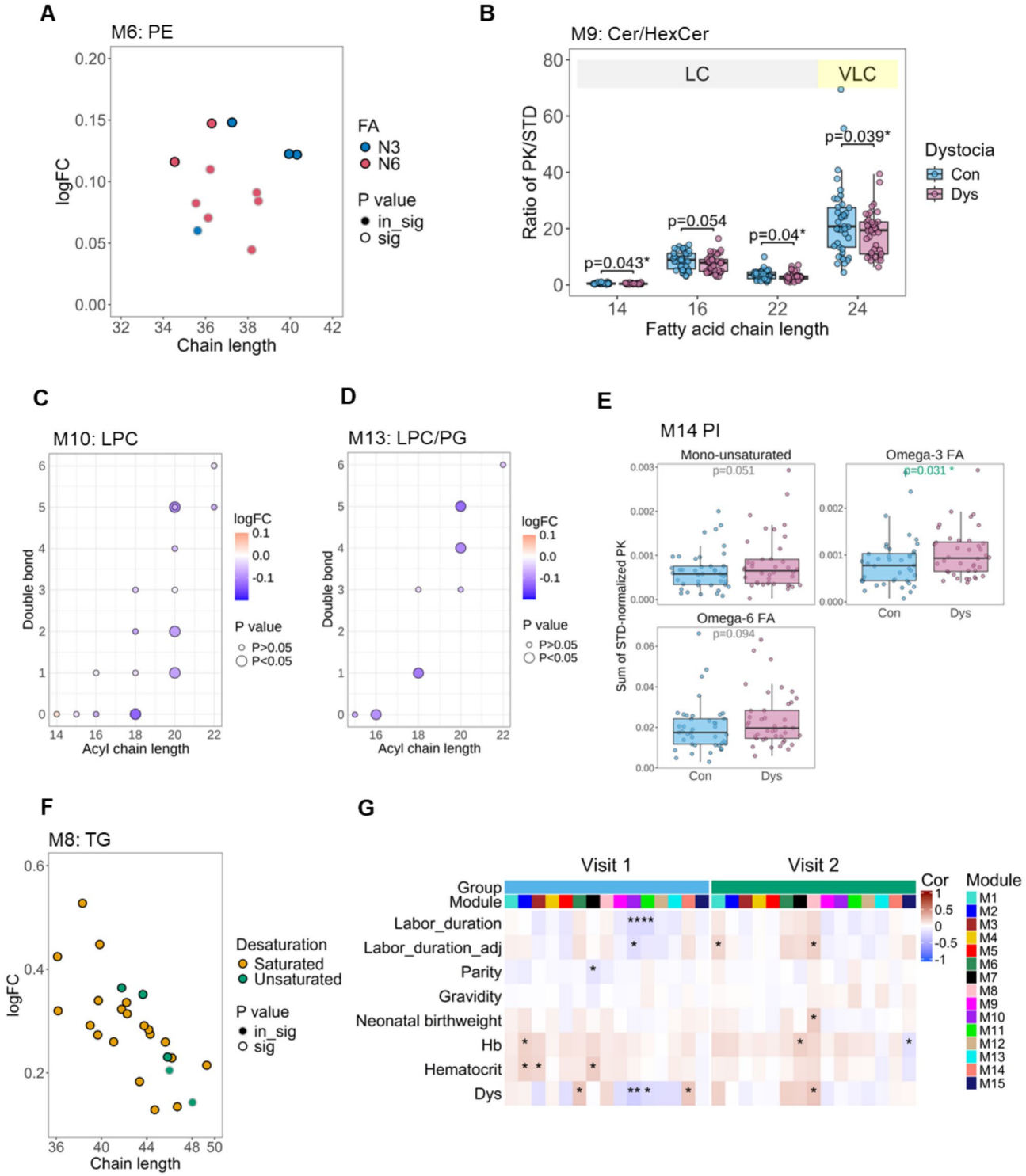

networks in early pregnancy, most notably a shift in triglyceride module affiliations and a reorientation of oxylipin and N-acylethanolamine relationships.

Beyond the reorganization of community membership, the module-module network topology itself differed markedly between groups in early pregnancy. The control group exhibited a total of 62 edges (connections) encompassing both positive and negative correlations, which reflects a more balanced and complex interaction among modules (Fig. 3C,D). In contrast, the dystocia group displayed only 46 edges, all of which were positive, indicating a loss of negative correlations and suggesting a disruption in regulatory balance. At the lipid class level, the dystocia group showed reduced net abundance of LPC, Cer, and SM at visit 1. Modules enriched in these lipid classes (LPC enriched M10 and M13; SM/Cer enriched M3, M5, M9) also exhibited fewer connections to other modules, indicating diminished network integration and potential decoupling from broader lipidomic interactions.

◀**Fig. 4**. Lipid modules associated with dystocia and their correlation with clinical outcomes. The bubble plot illustrating the log2 fold changes in lipid species between the dystocia and comparison group for (**A**) PE lipid species in module M6 and (**F**) TG species in module M8. Each point is plotted against total carbon length. Different colors represent the fatty acyl chains here: orange for saturated fatty acids; green for mono-unsaturated fatty acids (N9); blue for omega-3 (N3) fatty acids and red for omega-6 (N6) fatty acids. The black stroke indicates fold changes that achieves the statistical significance ($p < 0.05$). (**B**) Boxplots shows the ratio of peal area (PK)/internal standards(STD) of long chain (LC) and very long chain (VLC) Cer/HexCer in serum samples from comparison (Con) and dystocia (Dys) group across fatty acyl chain ranging from 14–24. $p < 0.05$ indicates statistical significance between group means using t-test. Bubble plot of carbon chain length vs. double bond for LPC lipid species in modules M10 (**C**) and M13 (**D**), showing log2 fold changes (dystocia/comparison). The intensity of the color gradient indicates the magnitude of the log2 fold change, while the size of the bubbles represents statistical significance. Boxplots of individual subjects within the PI lipid class of module M14, showing the sum of internal standards-normalized peak areas for the Comparison and Dystocia groups. Desaturation levels and carbon length by lipid class, and boxplots of individual subjects in the Comparison and Dystocia groups for different sub-lipid classes within the PI lipid class of module M14, shown in panels (**E**). (**G**) Heatmap showing the correlation results between clinical outcomes and lipid modules in the participants WGCNA was conducted using lipidomics data derived from all participants in African-American women cohort (n = 172; Visit 1: n = 82; Visit 2: n = 76; 72 participants attended both visits.). * $p < 0.05$; ** $p < 0.01$; *** $p < 0.001$. Labor_duration_adj: labor duration adjusted for parity and onset labor type. Hb: Hemoglobin.

At visit 2, modular community structures diverged notably between groups. In the control group, community 1 comprised modules M1, M2, M4, M5, M6, M7, M8, and M14, while community 2 comprised modules M3, M9, M10, M11, and M13. Conversely, in the dystocia group, ChE/SM-enriched module M3 shifted to community 1 whereas ether-linked PC/PE-enriched module M4 and PI-enriched module M14 was reassigned to community 2. Notably, module M2 was directly connected with module M9 in dystocia group, but not in the control group. Additionally, module M10 displayed reduced connectivity in the dystocia group, interacting with only module M13, while had broader associations with modules M3, M7, M9, M11 and M13 in the control group. Despite these topological differences, the total number of edges remained comparable and inter-community overlap was observed between the groups (Con: 50; Dys: 48) (Fig. S9A,B).

Thus, lipid co-expression network analysis identified 15 lipid modules across the cohort, of which five were significantly associated with labor dystocia in early pregnancy, characterized by elevated polyunsaturated PE and omega-3 PI, and reduced long-chain ceramides and LPC species, and one module (M8) featuring elevated saturated triglycerides in late pregnancy. Community structure analysis further revealed that labor dystocia was associated with a fundamental reorganization of inter-module relationships, including reduced network complexity, loss of negative regulatory correlations, and reassignment of key lipid class-enriched modules to different communities, with these topological differences being more pronounced in early than late pregnancy.

Network analysis of lipidomics associated with labor duration

After identifying lipid networks associated with a labor dystocia phenotype in the previous analysis, we next used a correlation-based approach to examine associations between the lipid co-expression modules and secondary clinical outcomes (neonatal birthweight, labor duration, hematocrit and hemoglobin) and active phase labor duration in participants at each visit, after adjusting for the influence of parity and mode of labor onset (Fig. 4G). Overall, we found that in visit 1 sera, modules M10 and M11 were significantly and negatively correlated with labor duration (M10: r = − 0.23, $p = 0.003$; M11: r = − 0.23, $p = 0.003$). This association remained for M10 after adjusting for parity and mode of labor onset (r = − 0.20, $p = 0.01$). Consistently, these two modules had significant association with dystocia cases (M10: r = − 0.30, $p = 0.005$; M11: r = − 0.22, $p = 0.048$). At visit 2, module M8 had stronger associations with adjusted labor duration (adjusted for parity and mode of onset, r = 0.20, $p = 0.02$), neonatal birthweight (r = 0.21, $p = 0.02$), and dystocia cases (r = 0.24, $p = 0.03$). Module M1 also showed a positive correlation with adjusted labor duration (r = 0.17, $p = 0.03$).

Together, these two network analyses of the labor dystocia phenotype and labor duration converge on several key modules. Both approaches consistently implicated M10 (LPC-enriched) in early pregnancy and M8 (saturated TG-enriched) in late pregnancy as central to labor dystocia, with M10 showing reduced abundance in dystocia cases and negatively correlating with labor duration, and M8 showing elevated abundance in dystocia and positively correlating with labor duration and neonatal birthweight. In late pregnancy, M1 (TG-enriched) also emerged as positively correlated with labor duration in the clinical correlation analysis, complementing the community-level finding that TG-enriched modules shifted community membership in dystocia, collectively pointing to dysregulated triglyceride metabolism in late pregnancy as a feature of prolonged labor. Overall, the two analyses reinforce each other in identifying disrupted LPC and ceramide metabolism in early pregnancy and aberrant triglyceride accumulation in mid pregnancy as the most consistent lipidomic signatures of labor dystocia.

Longitudinal lipidome changes across pregnancy and labor dystocia

We were also interested in examining whether longitudinal changes of the lipidome from early to late pregnancy were associated with labor dystocia. For this analysis, we included lipidomic data from visit 2 for the same participants who were also present at visit 1 in the analysis (72 participants, Con: n = 35; Dys: n = 37), unless otherwise specified (Fig. 1B). To evaluate lipidomic differences between labor dystocia groups longitudinally

across both prenatal visits, we conducted differential expression (DE, Visit 1: n = 82; Visit 2: n = 76) and difference of difference (DoD, n = 72 case/control participants with both a visit 1 and visit 2 sample) analysis as descriptive tools, rather than to develop predictive signatures. The DoD method first calculates the difference between two visits within the same group (within-group visit difference) and then assesses the difference in these visit-specific changes between groups (between-group difference). Using an UpSet plot (Fig. 5A), we visualized the overlap of lipid changes across multiple comparisons.

In the dystocia group, 371 lipid species showed significant changes across visits. Among these, the lipid species contributing specifically to the within-group visit difference (Dys_V2 vs. Dys_V1) were predominantly from the SM and Cer lipid classes. In contrast, the control group exhibited significant changes in 331 lipid species, with the group-specific visit difference primarily involving PC lipids. A total of 185 lipid species were shared between the two within-group visit comparisons, most of which belonged to the TG lipid class, followed by PC lipid class. The DoD analysis identified 54 lipids with significant changes in these between-group differences in visit-specific changes ((Dys_V2 – Dys_V1) – (Con_V2 – Con_V1)), with approximately half belonging to the TG lipid class. Interestingly, although both dystocia and control groups showed an increase in lipid levels at visit 2 compared to visit 1, the dystocia group exhibited a greater magnitude of change, resulting in a significant difference in the visit-specific group comparison (Fig. 5B).

Examination of individual lipid species within the dystocia-associated modules corroborated and further refined the network-level findings, revealing specific structural features that distinguished dystocia from control groups across pregnancy. Consistent with network analysis, a group of TG species from M8 module showed greater increase across pregnancy in the dystocia compared to the control group. Differentiating TG species were characterized by the presence of one medium-chain or short-chain fatty acid, with none of the fatty acids exceeding 18 carbons in length. Thus, shorter chain lengths of TGs are potentially associated with an increased risk of dystocia. In contrast, PCs associated with module M2, M4, and M6, all of which were primarily polyunsaturated PCs, were significantly elevated in the control group across pregnancy, while these same species exhibited the opposite direction in dystocia group, resulting in significantly lower levels in dystocia group compared to the control group. Moreover, ten lipids were significantly different between Dys and Con groups at visit 1; however, these differences were no longer evident at visit 2. Interestingly, the same lipids exhibited significant longitudinal changes across visits between groups, with the direction of change opposite to that observed at visit 1. Except for Hex1Cer(d18:1_16:0), all were phospholipids (Fig. S10A). There were seven lipids that consistently differed between Dys and Con groups at both visits, indicating persistent group-specific alterations (Fig. S10B). Notably, dynamic changes in PC(36:5) across pregnancy were associated with a greater likelihood of labor dystocia. A recurring theme among the identified predictors was the enrichment of phosphatidylcholines (PCs) containing 36 carbon atoms, suggesting incorporation of oleic acid, a major product of de novo lipogenesis. Additionally, TGs containing oleic acid (C18:1) exhibited a greater magnitude of increase during pregnancy in the labor dystocia group compared with the control group (Fig. 5B).

To capture the overall trajectory of lipidomic change across pregnancy rather than differences at individual time points, lipid set enrichment analysis was applied to examine lipid class- and module-level patterns associated with the rate and direction of lipid abundance change between early and late pregnancy in dystocia versus control groups. As shown in Fig. 6D, the lipid set enrichment analysis revealed distinct lipid class-level patterns in the DoD comparison. TG were positively enriched, indicating higher relative abundance, whereas PC and PI exhibited a negative enrichment, reflecting comparatively smaller changes. For PC, group differences were more pronounced at visit 1 and narrowed by visit 2, while changes across visits within Dys group remained modest. This suggests that the negative shift for PC does not imply depletion; rather, PC increased at a slower rate relative to Con group, as illustrated in Fig. 6F. Consistently, module level analysis showed that TG-enriched modules (M1, M7, M8) were positively enriched in dystocia sera, while modules predominantly composed of phospholipids including PC, PE, and PI (M2, M4, M6, M14), were negatively enriched (Fig. S10C). Together, these findings reveal a more profound divergence in lipidomic trajectories between labor dystocia and control groups during pregnancy. To explore visit-specific within-group differences while minimizing overestimation of model performance, we applied a machine learning pipeline with fully nested cross-validation, partitioning the dataset into training and testing sets at each fold. We initially considered 118 lipids showing significant changes across visits (26 lipids) or between groups at visit 1 (48 lipids) and visit 2 (44 lipids), based on Wilcoxon tests ($p < 0.05$). These lipids were incorporated into a binomial generalized linear model (GLM) to examine their potential association with dystocia outcomes. Following LASSO-based feature selection performed exclusively within the training data of each fold, 29 lipids were retained, corresponding to the lowest mean squared error (0.125) in nested cross-validation (Fig. S11A). sPLS-DA applied to these selected lipids improved separation between groups compared with models using data from only visit 1 or visit 2 (Figs. 2A, S5F, 6A). Ranking lipids by VIP scores and focusing on the top 20 provided an exploratory assessment of their discriminative potential, yielding a nested cross-validated ROC AUC of 0.733 (95% CI 0.447–0.884) (Fig. 6B,C). These findings indicate preliminary lipid signatures that may distinguish control and dystocia cases, requiring independent external validation in the future.

To investigate associations with labor duration, we extended the analysis by integrating these lipids with clinical variables, including BMI, gravidity, parity, gestational age at sampling (GA_time), and type of labor onset, by a stepwise regression model. Significant predictors of labor duration included ChE(20:4) + H, PC(40:8) + H, PC(35:5) + H, and PC(18:2_18:2) + H at visit 1; TG(4:0_16:0_18:2) + NH4 and LPC(20:1) + H at visit 2; and LPC(18:0) + H, oleic acid, and PC(34:2) + H as longitudinal predictors across visits (all $p < 0.05$; Table 2). BMI was significant in this analysis but was excluded from odds ratio calculations due to high multicollinearity (Fig. S11B). These predictors were further assessed using binomial regression to estimate odds ratios. While some estimates were affected by inter-individual variability, the overall patterns were consistent and informative. At the individual-visit level, PC(35:5), PC(40:8), PC(36:5), PC(18:2_18:2), TG(4:0_16:0_18:2) were associated with

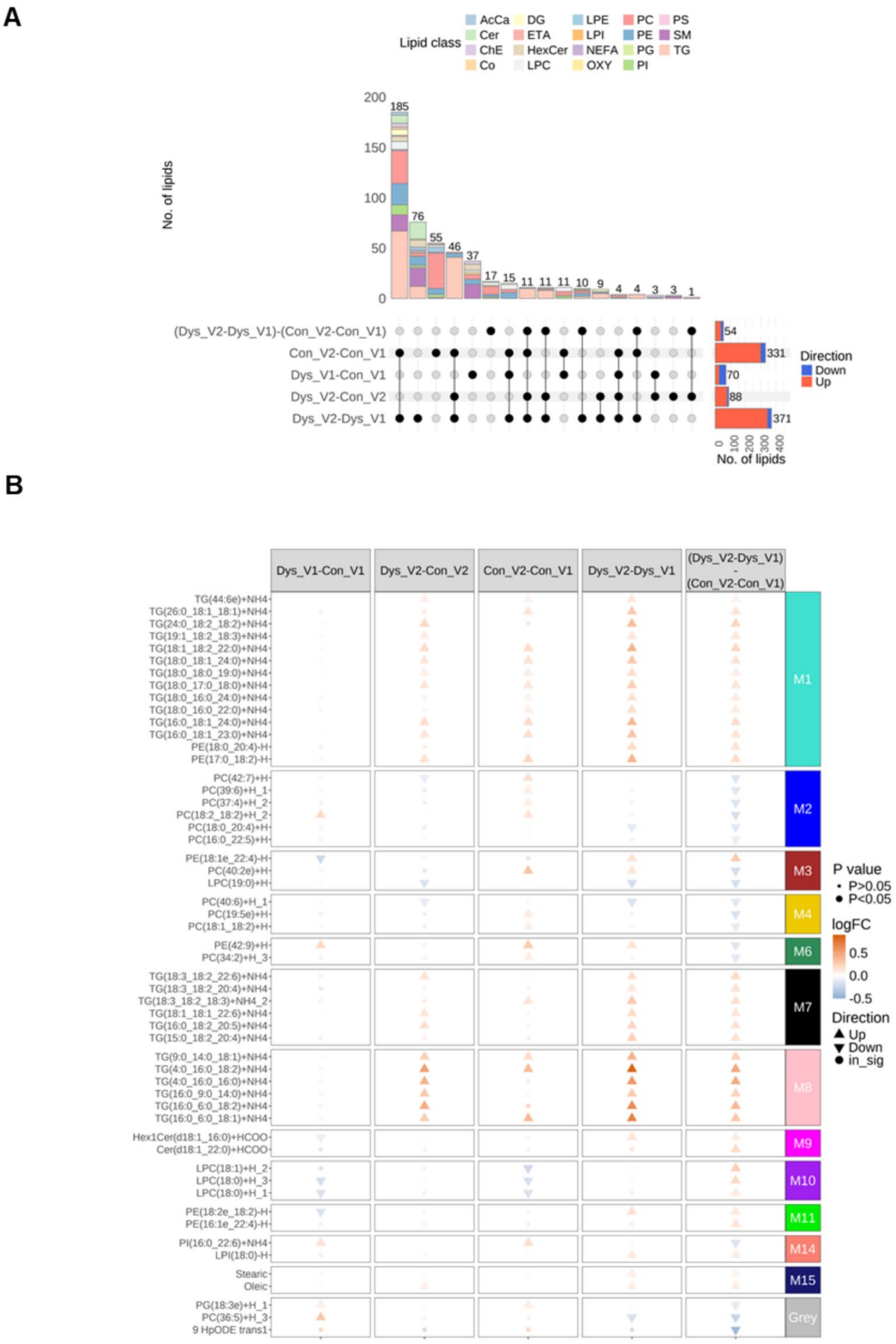

Fig. 5. The serum lipidomes during early-late pregnancy. (**A**) The upset plot illustrates the number of significant differences of lipid species from DE and DoD analysis between groups at both visits. The lipids with significant changes across five comparisons. (**B**) The panel highlights selected lipids species that are significantly changed in DoD analysis. Each lipid is represented by a symbol whose color reflects the $\log_2$ fold change (logFC), ranging from blue (decreased abundance) to red (increased abundance). The shape of the symbol conveys statistical significance and directionality: triangles indicate significant changes ($p < 0.05$), with upward-pointing triangles for increases and downward-pointing triangles for decreases, while circles denote non-significant changes ($p > 0.05$). Additionally, symbol size corresponds to the level of statistical significance, with larger symbols representing $p < 0.05$ and smaller symbols representing $p > 0.05$. The number of participants: Visit 1: n = 82; Visit 2: n = 76; 72 participants attended both visits.

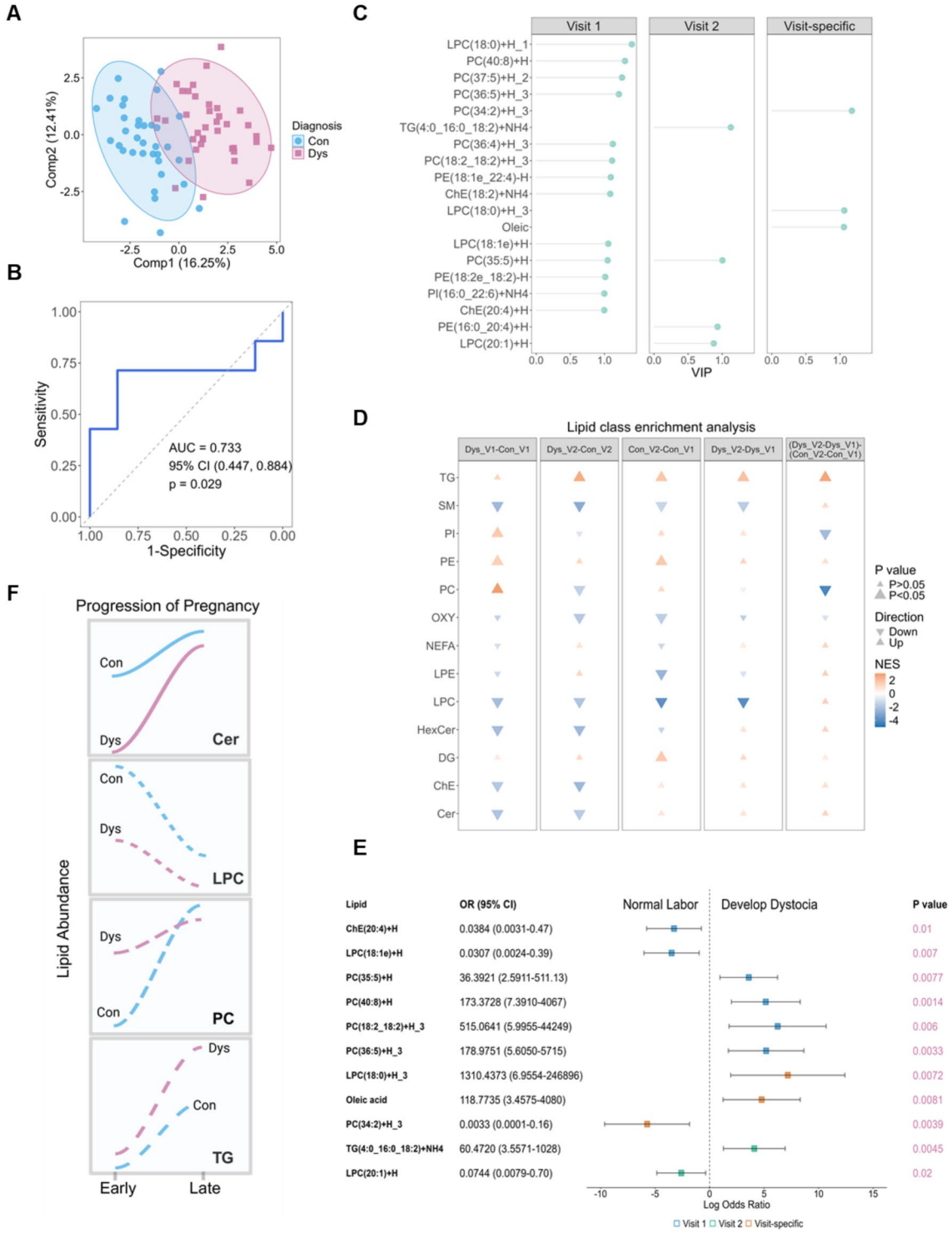

increased risk of labor dystocia, whereas ChE(20:4), PC(34:2), LPC(18:1e), and LPC(20:1) were linked to more rapid labor outcomes (Fig. 6E).

Overall, longitudinal lipidomic analysis revealed that labor dystocia was characterized by a greater increase in short-chain and oleic acid-containing TGs alongside a slower accumulation of polyunsaturated PCs across pregnancy, consistent at both the lipid-species and module levels. Integrating longitudinal and visit-specific lipid changes into the modeling framework provided preliminary evidence for potential discriminatory patterns, with specific PCs, cholesterol esters, and oleic acid emerging as candidate predictors of dystocia risk. These results underscore the value of examining dynamic lipid trajectories rather than static single-visit measurements, while emphasizing that findings remain exploratory until validated in independent cohorts.

◀**Fig. 6**. Potential serum lipid signatures distinguishes dystocia from normal labor outcomes. (**A**) PLSDA plot showing separation between Con and Dys groups based on lipidomic data after feature selection. **(B)** ROC curve based on top 20 VIP lipids, demonstrating better classification performance with an AUC of 0.733 (95% CI 0.447–0.884) by nested cross validation . **(C)** VIP scores from PLS-DA highlighting key lipids across Visit 1, Visit 2, and visit-specific changes. Untargeted lipidomic data were grouped by lipid classes and then evaluated for significance for multiple comparisons using enrichment analysis modified from fgsea R package. The results at lipid class level is shown in **(D)**. The direction of the triangle indicates log2 fold changes (LogFC)/ the normalized enrichment scores (NES) towards an increase (Up) or a decrease (Down). Larger triangle sizes indicate *p* values less than 0.05. LogFC/NES are presented using a color scale from negative (blue) to positive (red). The range of scale is determined by the minimum and maximum LogFC/NES. **(E)** Forest plot showing odds ratios (OR) and 95% confidence intervals (CI) for selected lipids and clinical traits associated with labor outcomes. Significant predictors ($p < 0.05$) are indicated. **(F)** The summary of dynamic changes in lipid classes during pregnancy. Oleic acid-containing PC and TG species were included in regression model to capture metabolic shifts. Total Cer and LPC species were used in regression model. Participants: n = 72.

Characteristic	Type	Beta	95% CI	*p* value
BMI_first	Clinical	36.95	14.17, 2.607	**0.012**
BMI_late	Clinical	− 23.41	15.16, − 1.544	0.128
ChE(20:4) + H	Visit 1	− 954.08	225.27, − 4.235	**< 0.001**
LPC(18:1e) + H	Visit 1	409.05	249.72, 1.638	0.107
PC(35:5) + H	Visit 1	− 175.93	68.19, − 2.58	**0.012**
PC(40:8) + H	Visit 1	776.82	267.49, 2.904	**0.005**
PC(18:2_18:2) + H_3	Visit 1	392.7	107.79, 3.643	**< 0.001**
PC(36:5) + H_3	Visit 1	146.12	91.79, 1.592	0.117
LPC(18:0) + H_3	Visit-specific	129.76	56.03, 2.316	**0.024**
Oleic acid	Visit-specific	72.32	32.5, 2.226	**0.030**
PC(34:2) + H_3	Visit-specific	− 151.23	38.88, − 3.889	**< 0.001**
TG(4:0_16:0_18:2) + NH4	Visit 2	168.27	48.62, 3.461	**0.001**
LPC(20:1) + H	Visit 2	− 730.77	271.74, − 2.689	**< 0.001**

Table 2. Longitudinal prenatal predictors for active phase labor duration using general mixed regression model (N = 72). *CI* confidence interval Type: Clinical = clinical traits; Visit 1 = The difference between Dys and Con groups at visit 1; Visit 2 = The difference between Dys and Con groups at visit 2; Visit-specific = The changes within the group during early to late pregnancy Beta: Coefficients Table reflects subjects with paired samples at Visit 1 and Visit 2 (n = 72 participants). GA_time: The duration between samples collection times at visit 1 and visit 2 in scale of gestation time in week BMI_first: BMI was calculated at visit 1 BMI_late: BMI was calculated at hospital admission for birth Active phase labor duration calculated as the time to complete cervical dilation (10 cm) for participants with either induced (4–10 cm dilation) or spontaneous labor onset (5–10 cm), based on clinician cervical examination.

Discussion

In this study, we investigated differences in the circulating prenatal lipidome among African American women with term labor dystocia compared to those with rapid labor progression, with cases carefully matched on maternal age, parity, maternal BMI, and mode of labor onset, the primary determinants of labor duration. All participants were cared for by the same provider group across two hospitals in the same geographic area, reducing provider-level bias. Among those with labor induction, there were no differences in initial cervical dilation, a key factor increasing risk for labor arrest[24]. As expected, labor dystocia cases were more likely to receive interventions meant to speed labor progression (amniotomy), to address pain during labor (epidural), and to experience labor complications associated with longer labor duration (infection, cesarean).

Using comprehensive untargeted lipidomics, lipid co-expression network analysis, and dynamic trajectory modeling across two prenatal time points, we identified several lipidomic signatures that were altered when comparing labor dystocia to rapid labor well before delivery. Our results suggest that labor dystocia is associated not only with isolated quantitative lipid differences, but with a fundamental reorganization of lipid metabolic networks characterized by disrupted phospholipid homeostasis in early pregnancy and progressive triglyceride accumulation across gestation.

Phospholipid dysregulation in pregnancy

Among the most consistent findings across all analyses in this study was the reduction of lysophosphatidylcholines (LPCs) in women who subsequently experienced labor dystocia, which we saw as early as 8–14 weeks' gestation (visit 1). LPC species were significantly reduced at the lipid class level, enriched in dystocia-associated modules M10 and M13, and negatively correlated with labor duration after adjusting for parity and mode of labor onset.

These findings are consistent with Saadat et al.[25], who reported significant decreases in circulating LPE and LPC over the course of pregnancy in African American women, and we corroborate this pattern across all participant sera, with LPC decreasing from early to late pregnancy. However, in our study the dystocia group ended at substantially lower LPC levels by the early third trimester than the rapid labor comparison group. Notably, circulating LPC serves as the primary substrate for autotaxin (ATX)-mediated production of lysophosphatidic acid (LPA)[26]. In a rat model, LPA was found to be a bioactive lipid that augments myometrial contraction force just before parturition, working with prostaglandins cooperatively[27]. Thus, the sustained reduction of circulating LPC observed among dystocia cases may reflect impaired substrate availability for ATX-driven LPA synthesis, potentially compromising the uterotonic signaling necessary for efficient labor progression at term. Future validations studies featuring enzymatic assays or tissue-level studies are needed to further clarify possible LPC-related mechanisms of impaired uterine contractility.

Ceramides, particularly long-chain and very long-chain species (C22 and C24) in the M9 module, were also significantly reduced in early pregnancy among labor dystocia cases, followed by rapid increases in late pregnancy. Very long-chain ceramides are structural membrane components with roles in cellular stress, apoptosis, and inflammatory signaling[28]. Their co-reduction with sphingomyelin, along with diminished network connectivity of sphingolipid-enriched modules, suggests a broader suppression of sphingolipid metabolism rather than isolated ceramide depletion[29]. The functional consequences of reduced circulating ceramide and sphingomyelin in the dystocia group may extend to myometrial contractile machinery through their role in caveolar membrane composition. Caveolae, which are cholesterol- and sphingolipid-rich plasma membrane invaginations abundant in smooth muscle cells, serve as critical signaling microdomains in the myometrium, housing key contractile regulators including oxytocin receptors[11]. Disruption of caveolar sphingolipid content has been shown to impair oxytocin signaling strength at these microdomains[30]. Thus, the broader suppression of sphingolipid metabolism observed in early pregnancy among dystocia cases may contribute to inefficient uterine contractility through disruption of caveolar membrane integrity and its downstream signaling capacity.

The elevation of polyunsaturated PE species in the labor dystocia group during early pregnancy, particularly those containing arachidonic acid (AA, C20:4) and docosahexaenoic acid (DHA, C22:6) in the M6 module, is also noteworthy. PE serves as a substrate for phospholipase-mediated release of polyunsaturated fatty acids subsequently converted to eicosanoids and other bioactive mediators, so elevated PE-AA and PE-DHA may indicate increased substrate availability for inflammatory lipid mediator production relevant to uterine contractility[31,32]. Similarly, the M14 module showed selective elevation of omega-3 FA-containing phosphatidylinositol (PI) species in the dystocia group. To the authors' knowledge, this is the first report of altered PI abundance in labor dystocia. PI comprises roughly 1.5% of circulating glycerophospholipids and serves as a precursor for phosphoinositides involved in smooth muscle contraction and calcium handling[33]. Importantly, PI, primarily 18:0–20:4 PI, is a well-recognized source of arachidonic acid released from the amnion and chorion during early labor, which serves as the biological precursor for prostaglandins triggering cervical ripening and uterine contractions[34]. Despite elevated PI levels in the dystocia group, serum prostaglandin levels were not increased, suggesting a possible disconnect between precursor availability and downstream signaling, or differences between circulating and organ-level availability of key mediators of labor. In a rat model of obesity, decreased uterine PUFAs and increased omega-6 PUFAs were associated with reduced uterine contraction strength and coordination at term[22,23]. Future studies more closely examining dietary omega-3 and omega-6 intake in relation to labor duration, contraction strength, and coordination would be valuable[35].

Taken together, the decreased abundance of LPC and the increased circulating abundance of phospholipids containing PUFA suggests that glycerophospholipid remodeling may have been impacted in labor dystocia cases. It is well documented that membrane phospholipids are reservoirs of bioactive PUFA, specifically arachidonic acid (ARA) and docosahexaenoic acid (DHA)[36]. Hydrolysis of these membrane phospholipids produces a lysophospholipid and a newly liberated PUFA, that is shunted into several pathways. One such pathway is the FAAH pathway, whereby ARA is used as the biosynthetic precursor of endocannabinoids anandamide (AEA) and arachidonoyl glycerol (2-AG), two key components of the delicate endocannabinoid system (ECS) that is required for uterine activation during parturition[37]. While we did observe statistically significant differences in lysophospholipids, we did not observe differences in the abundance of AEA and 2-AG. We speculate that this is due to the highly utilization of these lipid species during delivery.

Triglyceride accumulation in late pregnancy

In contrast to the phospholipid-dominated early pregnancy picture of labor dystocia, late pregnancy lipidomics differentiating labor dystocia was characterized by differential triglyceride accumulation. Both groups had comparable TG levels in early pregnancy, but by late pregnancy, labor dystocia cases showed a sharp increase relative to controls. The saturated TG-enriched M8 module was the only module significantly elevated in late pregnancy dystocia cases, and it was also positively correlated with labor duration and neonatal birthweight. Longitudinal analysis further confirmed that short-chain and oleic acid-containing TG species showed a greater magnitude of increase across pregnancy in the dystocia group. Maternal TGs have been linked to increased risks of infant macrosomia and gestational diabetes mellitus, and dysregulated circulating TGs are strongly associated with obesity and metabolic syndrome in pregnancy[38,39]. Although there was no significant difference in neonatal birthweight between groups in this study, the correlation between the saturated TG module and birthweight suggests the metabolic milieu of dystocia may have broader implications for fetal growth and perinatal outcomes.

By contrast, PC levels were higher in early pregnancy in dystocia cases than in controls, but by late pregnancy the two groups converged following a dramatic PC increase in control sera. This pattern of PC increasing more slowly in the labor dystocia group reflects a relative rather than absolute depletion, and is consistent with prior findings from this group demonstrating perturbed fatty acid metabolism in pregnancies ending in labor

dystocia[13], corroborated by others using metabolomics and epigenetic profiling[14]. Specifically, dystocia case sera became depleted of polyunsaturated fatty acids and enriched in TGs across pregnancy.

Oleic acid and de novo lipogenesis as a recurring theme

A recurring theme across the lipid features we found associated with labor dystocia was the incorporation of oleic acid (C18:1) into circulating PC and TG species. Oleic acid is the primary product of stearoyl-CoA desaturase-1 (SCD-1) and a marker of de novo lipogenesis[40]. We observed that it progressively increased across pregnancy with a significantly greater rise in the dystocia group by late gestation. Soldavini et al. showed that plasma oleic acid was associated with a pro-inflammatory metabolic state and increased risk for gestational diabetes, fetal overgrowth, and preeclampsia[41]. While dietary oleic acid is generally considered beneficial, increases in serum oleic acid during labor dystocia likely reflect pathophysiologic de novo synthesis rather than dietary intake, as the two are minimally correlated[42]. Future studies integrating detailed dietary intake with lipidomic profiling will be important to clarify whether diet represents a modifiable contributor to dystocia risk.

Network-level reorganization of lipid metabolism

Beyond individual lipid class differences, lipid co-expression network analysis revealed that labor dystocia was associated with a rewiring of lipid metabolic architecture in this sample. In early pregnancy, the dystocia group exhibited a simplified inter-module network with only 46 edges compared to 62 in controls, and a complete absence of negative regulatory correlations. The loss of negative associations, which are thought to reflect homeostatic reciprocal regulation of competing metabolic pathways[43], suggests a disruption in the regulatory balance of lipid metabolism rather than simply altered abundance. The shift in oxylipin and *N*-acylethanolamine module associations from ether-linked PE (in controls) to ester-linked polyunsaturated PE (in dystocia) suggests a reorientation of bioactive lipid mediator production with potential functional consequences for uterine contractility and immune regulation[44]. These network-level differences were more pronounced in early pregnancy, consistent with findings that the most significant metabolic divergence precedes the period of rapid fetal growth and third-trimester lipid accumulation[45].

Dynamic lipid trajectories as superior predictors of labor dystocia

A key translational finding is that integrating dynamic lipidomic changes across pregnancy with visit-specific differences substantially outperformed models using either time point alone. This underscores that the trajectory of lipid change, rather than any static snapshot, provides the most informative biological signal for dystocia risk. Among significant predictors of labor duration and dystocia risk were specific PC, SM, cholesteryl ester CE(20:4), and DG species, with the arachidonic acid-containing CE(20:4) further implicating altered AA storage and mobilization as a relevant pathway. Taken together, these model results and the network analysis converge on a coherent metabolic narrative: early disruption of phospholipid homeostasis, progressive triglyceride accumulation driven partly by de novo lipogenesis, and loss of regulatory network complexity collectively characterize the lipidomic trajectory toward labor dystocia.

Intrapartum interventions and pregnancy lipidome

As expected, intrapartum interventions including epidural analgesia, amniotomy, and intrapartum infection occurred at substantially different rates between groups, and while these were appropriately excluded as covariates, as they are consequences rather than causes of prolonged labor (Supplemental Table 11), their potential biological interactions with the lipid signatures we identified warrant discussion. Epidural analgesia, used in 97.7% of dystocia cases compared to 39.5% of controls, has been associated with alterations in inflammatory mediator profiles[46], which could theoretically influence some of the lipid signatures we observed. However, the direction of this effect is unlikely to explain our findings, as epidural use is itself a downstream response to prolonged painful labor rather than a determinant of the prenatal lipidome measured weeks before delivery. Similarly, intrapartum infection, an established complication of prolonged membrane rupture and labor, is known to activate phospholipase A2 and the arachidonic acid cascade[32], pathways already implicated in our findings. However, given that our lipidomic samples were collected at 8–14 and 24–30 weeks' gestation, well before the intrapartum period, these infections cannot have caused the prenatal lipidomic differences we report. Rather, we suggest that the shared underlying biology of dysregulated phospholipid metabolism and impaired prostaglandin signaling may predispose women both to the lipidomic profile we identified prenatally and to the intrapartum complications that accompany prolonged labor, representing parallel manifestations of the same underlying metabolic disruption rather than causal intermediaries.

Strengths and limitations

Strengths of this study include comprehensive untargeted lipidomic profiling, longitudinal sampling at two prenatal visits, careful case–control matching for known confounders, and a focus on an African American population at disproportionate risk for labor dystocia and adverse birth outcomes. Limitations include the use of manual cervical dilatation assessments, which can be different depending on the experience of the examiner[47], prompting calls for ultrasound assessment of cervical changes in situations where interobserver accuracy is critical, such as multi-site clinical trials for labor induction agents[48]. However, as all participants in this study labored at two hospitals in the same locale, where they were attended by the same set of residents and attendings operating under the same norms for cervical assessment, some but not all interobserver variation or error in cervical assessments for this study was minimized. An additional limitation was a relatively small sample size, which necessitates external validation before clinical application of these biomarkers; and the use of serum lipidomics, which reflects systemic lipid profiles rather than mechanistic activity in reproductive tissues. Also, this study did not integrate maternal diet or body composition into the current analyses; both are planned for a

forthcoming analysis on a nearly complete cohort. Finally, our targeted NEFA assay did not detect many PUFAs such as 20:5 and 22:6 or phosphatidylinositol phosphate lipids, likely due to low abundance.

Conclusion

By demonstrating distinct and dynamic lipidomic profiles in African American women with labor dystocia compared to those with rapid labor, this study highlights LPC, ceramide, PI, polyunsaturated PE, and oleic acid-containing TG and PC species as candidate biomarkers and mechanistic contributors to labor dystocia risk. These findings suggest that disrupted phospholipid and triglyceride metabolism may impair cervical ripening and uterine contractility, contributing to prolonged labor. Future work should validate these lipidomic signatures in larger, more diverse cohorts, integrate dietary and body composition data, and investigate mechanistic links between maternal lipid metabolism and labor physiology with the goal of informing early risk stratification and reducing obstetric inequities in maternal health.

Methods

Study design and population

This study utilized a case–control study design to identify maternal lipidomic biomarkers and networks describing term labor dystocia in serum samples from a group of African-American women who participated in the Emory University African American vaginal, oral, and gut microbiome in pregnancy cohort study (the parent study), which began recruitment in 2014[49]. That study included self-identified African American women ages 18 to 40 years, who carried a singleton pregnancy, and attended one of two clinics in Atlanta, GA, where they received care from a common group of physicians and midwives. All participants were healthy at study entry, with any chronic medical condition being an exclusion for study participation. Once confirming their informed consent for study participation being enrolled, participants had two in-person visits at 8–14 weeks' gestation and again at 24–30 weeks' gestation, where blood samples were collected for lipidomics analysis and processing.

For the current study, we focused on a cohort of women from the parent study who achieved term gestation (gestational age of at least 37 0/7 weeks on the day of delivery), and either completed the first stage of labor (reached 10 cm cervical dilation) or received a cesarean section for the indication of labor dystocia (N = 173). From this retrospective cohort, we selected cases exhibiting a labor dystocia phenotype and controls with the fastest quartile labors for a nested case–control arm of this study, with selected participants matched on maternal age, parity, mode of labor onset, and body mass index (N = 86) (Fig. 1B).

Institutional approval from Emory University was obtained for this study (protocol # 00,002,852), in addition to approval of data/sample use by the investigators of the parent study. All participants of this study provided informed consent for parent study participation and secondary use of their samples and data for follow-up studies. All methods carried out in this study were done so in accordance with relevant guidelines and regulations, as approved by the Emory University IRB.

Data collection

Socioeconomic variables were self-reported by participants and collected in medical records, including maternal age, educational background, partnership status, health insurance status, and household income. Medical record abstractions were performed in the parent study following labor and birth to capture all pregnancy outcomes, including complications occurring during or after pregnancy. Medical chart abstraction was completed by the research team using a standardized chart abstraction tool. To confirm the accuracy of medical chart abstractions, repeat medical record abstractions were completed by two experienced clinicians for 6.9% of the participants, with excellent agreement (> 95%) between members of the research team on all abstracted variables[50]. In parent study medical record abstractions, information was collected on participant's pre-pregnancy and delivery body mass index (BMI), gestational age at birth, and parity. Maternal BMI was calculated using measured height at the first prenatal visit, and patient report of pre-pregnancy weight. Gestational age at birth was calculated using date of delivery in relation to the date of last menstrual period and/or first trimester ultrasound. Parity was recorded as a discrete variable and categorized as nulliparous (parity < 1 previous vaginal birth of at least 20 gestational weeks) or multiparous (parity > 1 previous vaginal birth of at least 20 weeks) for analysis.

For the current study, expanded medical record abstractions were undertaken to obtain detailed information on each participant's labor course, including the date/time of contraction onset, intrapartum hospital admission, and birth. We also collected date/time and result of each cervical examination in labor, which were used to calculate the duration of first stage labor (contraction onset until 10 cm cervical dilatation) and active phase labor 4 cm–10 cm cervical dilatation for participants with labor induction, or 5 cm–10 cm cervical dilatation for participants with spontaneous on se to flabor.

Additionally, medical record information was collected on all labor interventions, including the use of medications (synthetic oxytocin, prostaglandins) or procedures (amniotomy, cervical catheter placement) intended to initiate or speed the course of labor, and complications (occiput posterior positioning or other malposition) known to slow labor progression. Then, cases of labor dystocia (n = 43) and comparison participants with the fastest labors (n = 43) were selected based upon highest vs. lowest tertile of ranked total labor duration, matching on parity, age, mode of labor onset (induction vs. spontaneous onset), and BMI[2].

Lipidomic analysis

Blood samples were drawn at visit 1 8–14 weeks of gestation and visit 2 (24–30 weeks of gestation). Serum was collected, processed immediately, and stored at − 80 °C between 2014 and 2017 (Fig. 1A). High-resolution untargeted lipidomic analysis and targeted lipidomic assays were performed to identify oxylipins, endocannabinoids, and non-esterified fatty acids in the stored serum samples. Sample preparation for these

lipidomic analyses was conducted using HPLC–MS spectrometry, following protocols outlined in our previous publications[38,51]. The data processing pipelines, including data filtering criteria, batch correction, and normalization methods, are detailed in the supplementary materials. Parameters for chromatography and mass spectrometry, along with the list of validated lipids, are provided in Tables S1–S9. For untargeted lipidomic hits, batch effects were minimized using quality control robust spline correction (QC-RSC) until quality control distribution was tightened to a single cluster (Fig. S1A,B). For targeted lipidomics, the batch effect was minimized after ComBat batch effect adjustment, and overall RSD was reduced for each metabolite (Fig. S1C–F).

Statistical analysis

In conceptualizing the causal pathway from prenatal lipidome to labor dystocia, the serum lipidomic profile is treated as the primary predictor of interest, with labor duration and labor dystocia as the outcomes (Supplemental Table 11). Several upstream variables, including parity, maternal age, BMI, gestational age at labor onset, and mode of labor onset, are recognized as independent determinants of labor duration that could confound the lipidome-dystocia relationship, and were addressed through case–control matching and covariate adjustment in multivariate models. Gestational diabetes was not controlled for, as this condition is plausibly downstream of the same dysregulated lipid metabolism that characterizes the dystocia group, thus inclusion as a covariate would risk over-adjustment by blocking part of the causal pathway of interest. Similarly, intrapartum variables including epidural analgesia and chorioamnionitis were not controlled for, as these arise during labor itself and therefore lie within the causal pathway between the prenatal lipid environment and the labor outcome rather than upstream of it. This causal structure supports the interpretation that the prenatal lipidomic differences we identified are not confounded by intrapartum events, but may instead reflect a shared underlying metabolic predisposition that manifests both in the prenatal lipidome and in the labor complications that accompany dystocia.

To determine significant abundance differences in lipids varying with the labor dystocia phenotype, normalized lipid profiles were used for multivariate statistical analysis. Briefly, the lipidomics data were normalized using log transformation followed by auto-scaling and adjusted for covariates, including age, body mass index, socioeconomic status, gestational age at birth, gestational weeks at sample collection, and neonate's sex at birth implemented with the limma[52] and stats R packages using a stepwise regression model if the R-squared value was greater than 0.01 (Fig. S2A). Next, we conducted weighted lipid co-expression network analysis (WGCNA) using the WGCNA R package[53] to cluster lipids into modules, with module eigengenes (MEs) correlated to clinical traits using Spearman correlation. Prior to WGCNA, the lipidomics dataset was pre-adjusted using the withinVariation() function in the mixOmics R package to account for within-subject variationin the full corhort. WGCNA was then performed usingthe adjusted data to construct a robust co-expression network, incorporating available visit 1 or visit 2 samples for each participant (314 samples from 172 participants). Lipid class enrichment within modules was assessed using over-representation analysis (ORA) with one-sided Fisher's exact tests, while lipid set enrichment analysis (LSEA) was performed on ranked datasets using the fgsea R package[54](Fig. 1B).

After normalization and characterization of the lipid co-expression network, we focused on participants selected for the labor dystocia case/control groups for further analyses (n = 86). First, we extracted the lipidomic samples for matched case–control participants who had lipidomic results from early pregnancy (visit 1) (n = 82). Prior to principal component analysis (PCA), significant differential lipids identified through univariate analysis were selected for use in subsequent multivariate analysis. PCA and sparse partial least squares discriminant analysis (sPLS-DA) were performed to identify significant lipids between groups at each study visit timepoint using the mixOmics R package[55].

Next, we focused on participants selected for the case/control groups who had lipidomic results from both pregnancy study visits (n = 72) for within-subject analyses. In this group, we first evaluated associations between individual clinical factors and active labor duration. Variables considered included onset of labor type, nulliparous status, gravity, BMI, and sampling time, and the final generalized linear models were used to assess the contribution of each factor. We also evaluated longitudinal lipid changes associated with labor duration in this group.

Next, building from the lipid co-expression network already characterized for the entire cohort, we conducted differential expression (DE, Visit 1: n = 82; Visit 2: n = 76) and difference-of-differences (DoD, n = 72) analyses using the limma R package to evaluate fold changes between groups of participants, according to their labor dystocia phenotype, at the same visit and across visits between groups, respectively[53,54]. Limma incorporates empirical Bayes moderation and applies false discovery rate (FDR) correction to account for multiple comparisons in these high-dimensional lipid analyses. For group-wise comparisons, we used chi-square or ANOVA followed by Tukey's honest significant difference test for multiple-group comparisons[52,55,56].

A fully nested cross-validation framework was used to obtain an unbiased estimate of the sPLS-DA model's exploratory discriminative performance. All analyses were conducted in R using mixOmics, pROC, and caret, with the outcome encoded as a binary factor ("0" = Con, "1" = Dys). In each outer fold of fivefold cross-validation with 5 repeats, feature selection was restricted strictly to the training data: lipids showing significant group differences (Wilcoxon test, $p < 0.05$) were retained, followed by binomial LASSO regression for additional dimensionality reduction. An sPLS-DA model was then trained on the LASSO-selected lipids, features were ranked by VIP scores, and the top 20 were used to refit the model within that fold. The held-out fold was excluded from all feature-selection and model-fitting steps and used solely for potential interests. Discriminative performance was quantified using ROC curves and AUC values, with overall performance summarized as the mean outer-fold AUC and their corresponding 95% confidence intervals. Performance of individual lipid features was further assessed using pROC and precrec, and all findings are interpreted as exploratory and hypothesis-generating pending external validation or repeated nested-CV evaluation of feature-selection stability[54,57]. Results were

visualized with ggplot2, network plots were generated using igraph, ggraph, and tidygraph, and eigenvector centrality was calculated to assess node influence within the network. Detailed information about all statistical methods is provided in the Supplementary Materials.

Data availability

The Emory University African American Vaginal, Oral, and Gut Microbiome in Pregnancy Cohort Study materials and dataset are maintained by project PI Dr. Anne Dunlop (amlang@emory.edu). The clinical and lipidomics datasets used to generate the findings of study can be requested directly by contacting: chih-yu.chen@emory.edu.

Code availability

All code used in this study was cited and described within the manuscript. Details of the code implementation, including algorithms and data processing scripts, are provided in the methods section and relevant figure legends. Additional information is available upon request from chih-yu@emory.edu.

Received: 26 November 2025; Accepted: 23 March 2026
Published online: 02 April 2026

References

1. Leonard, S. A., Main, E. K. & Carmichael, S. L. The contribution of maternal characteristics and cesarean delivery to an increasing trend of severe maternal morbidity. *BMC Pregnancy Childbirth.* **19**(1), 16 (2019).
2. Sandall, J. et al. Short-term and long-term effects of caesarean section on the health of women and children. *Lancet* **392**(10155), 1349–1357 (2018).
3. Spong, C. Y., Berghella, V., Wenstrom, K. D., Mercer, B. M. & Saade, G. R. Preventing the first cesarean delivery: summary of a joint Eunice Kennedy Shriver National Institute of Child Health and Human Development, Society for Maternal-Fetal Medicine, and American College of obstetricians and gynecologists workshop. *Obstet. Gynecol.* **120**(5), 1181–1193 (2012).
4. Barber, E. L. et al. Indications contributing to the increasing cesarean delivery rate. *Obstet. Gynecol.* **118**(1), 29–38 (2011).
5. Chu, S. Y. et al. Maternal obesity and risk of cesarean delivery: a meta-analysis. *Obes. Rev.* **8**(5), 385–394 (2007).
6. Vahratian, A., Siega-Riz, A. M., Savitz, D. A. & Zhang, J. Maternal pre-pregnancy overweight and obesity and the risk of cesarean delivery in nulliparous women. *Ann. Epidemiol.* **15**(7), 467–474 (2005).
7. Hautakangas, T., Palomaki, O., Eidsto, K., Huhtala, H. & Uotila, J. Impact of obesity and other risk factors on labor dystocia in term primiparous women: a case control study. *BMC Pregnancy Childbirth.* **18**(1), 304 (2018).
8. Tse, W. T. et al. Labor progress determined by ultrasound is different in women requiring cesarean delivery from those who experience a vaginal delivery following induction of labor. *Am. J. Obstet. Gynecol.* https://doi.org/10.1016/j.ajog.2019.05.040 (2019).
9. Gam, C. M. B. F. et al. Unchanged mitochondrial phenotype, but accumulation of lipids in the myometrium in obese pregnant women. *J. Physiol.* **595**(23), 7109–7122 (2017).
10. Frayn, K. N. *Metabolic Regulation: A Human Perspective* 3rd edn. (Wiley-Blackwell Pub, Chichester, Malden, 2010).
11. Carlson, N. S., Hernandez, T. L. & Hurt, K. J. Parturition dysfunction in obesity: time to target the pathobiology. *Reprod. Biol. Endocrinol. RB&E.* **13**(1), 135 (2015).
12. Carlson, N. S., Frediani, J. K., Corwin, E. J., Dunlop, A. & Jones, D. Metabolomic pathways predicting labor dystocia by maternal body mass index. *AJP Rep.* **10**(1), e68–e77 (2020).
13. Carlson, N. S., Frediani, J. K., Corwin, E. J., Dunlop, A. & Jones, D. Metabolic pathways associated with term labor induction course in African American women. *Biol. Res. Nurs.* **22**(2), 157–168 (2020).
14. Prifti, K. K. et al. Obese mice have decreased uterine contractility and altered energy metabolism in the uterus at term gestation†. *Biol. Reprod.* **111**(3), 678–693 (2024).
15. Hornburg, D. et al. Dynamic lipidome alterations associated with human health, disease and ageing. *Nat. Metab.* **5**(9), 1578–1594 (2023).
16. Jones, D. P. Redefining oxidative stress. *Antioxid. Redox Signal.* **8**(9–10), 1865–1879 (2006).
17. Abu Bakar, M. H. et al. Metabolomics—THE complementary field in systems biology: a review on obesity and type 2 diabetes. *Mol. BioSyst.* **11**(7), 1742–1774 (2015).
18. Jones, D. P., Park, Y. & Ziegler, T. R. Nutritional metabolomics: Progress in addressing complexity in diet and health. *Annu. Rev. Nutr.* **32**, 183–202 (2012).
19. Patti, G. J., Yanes, O. & Siuzdak, G. Innovation: metabolomics: the apogee of the omics trilogy. *Nat. Rev. Mol. Cell Biol.* **13**(4), 263–269 (2012).
20. Xie, B., Waters, M. J. & Schirra, H. J. Investigating potential mechanisms of obesity by metabolomics. *J. Biomed. Biotechnol.* **2012**, 805683 (2012).
21. Quehenberger, O. et al. Lipidomics reveals a remarkable diversity of lipids in human plasma. *J. Lipid Res.* **51**(11), 3299–3305 (2010).
22. Muir, R. et al. Modelling maternal obesity: the effects of a chronic high-fat, high-cholesterol diet on uterine expression of contractile-associated proteins and ex vivo contractile activity during labour in the rat. *Clin. Sci. (Lond.)* **130**(3), 183–192 (2016).
23. Muir, R. et al. Maternal obesity-induced decreases in plasma, hepatic and uterine polyunsaturated fatty acids during labour is reversed through improved nutrition at conception. *Sci. Rep.* **8**(1), 3389 (2018).
24. Jakub, M., Marta, M., Jagoda, G., Kamila, G. & Stanislaw, G. Is Unfavourable cervix prior to labor induction risk for adverse obstetrical outcome in time of universal ripening agents usage? Single center retrospective observational study. *J. Pregnancy.* **2020**, 4985693 (2020).
25. Saadat, N. et al. Changes in lipid profiles with the progression of pregnancy in Black women. *J. Clin. Med.* https://doi.org/10.3390/jcm13102795 (2024).
26. Okudaira, S., Yukiura, H. & Aoki, J. Biological roles of lysophosphatidic acid signaling through its production by autotaxin. *Biochimie* **92**(6), 698–706 (2010).

27. Nagashima, S. et al. Lysophosphatidic acid stimulates rat uterine contraction in vitro. *J. Reprod. Dev.* **69**(3), 163–169 (2023).
28. Hannun, Y. A. & Obeid, L. M. Sphingolipids and their metabolism in physiology and disease. *Nat. Rev. Mol. Cell Biol.* **19**(3), 175–191 (2018).
29. Taniguchi, M. & Okazaki, T. The role of sphingomyelin and sphingomyelin synthases in cell death, proliferation and migration-from cell and animal models to human disorders. *Biochem. Biophys. Acta.* **1841**(5), 692–703 (2014).
30. Padol, A. R. et al. Hypercholesterolemia impairs oxytocin-induced uterine contractility in late pregnant mouse. *Reproduction* **153**(5), 565–576 (2017).
31. Hanna, V. S. & Hafez, E. A. A. Synopsis of arachidonic acid metabolism: a review. *J. Adv. Res.* **11**, 23–32 (2018).
32. Besenboeck, C., Cvitic, S., Lang, U., Desoye, G. & Wadsack, C. Going into labor and beyond: phospholipase A2 in pregnancy. *Reproduction* **151**(6), R91-r102 (2016).
33. Lydic, T. A. & Goo, Y. H. Lipidomics unveils the complexity of the lipidome in metabolic diseases. *Clin. Transl. Med.* **7**(1), 4 (2018).
34. Zhang, F., Sun, K. & Wang, W. S. Identification of a feed-forward loop between 15(S)-HETE and PGE2 in human amnion at parturition. *J. Lipid Res.* **63**(11), 100294 (2022).
35. DiNicolantonio, J. J. & O'Keefe, J. The importance of maintaining a low omega-6/omega-3 ratio for reducing the risk of autoimmune diseases, asthma, and allergies. *Mo Med.* **118**(5), 453–459 (2021).
36. Gabbs, M., Leng, S., Devassy, J. G., Monirujjaman, M. & Aukema, H. M. Advances in our understanding of Oxylipins derived from dietary PUFAs. *Adv. Nutr.* **6**(5), 513–540 (2015).
37. Kozakiewicz, M. L., Grotegut, C. A. & Howlett, A. C. Endocannabinoid system in pregnancy maintenance and labor: a mini-review. *Front. Endocrinol. (Lausanne).* **12**, 699951 (2021).
38. Huneault, H. E. et al. Lipidome changes associated with a diet-induced reduction in hepatic fat among adolescent boys with metabolic dysfunction-associated steatotic liver disease. *Metabolites* https://doi.org/10.3390/metabo14040191 (2024).
39. Song, X. et al. High maternal triglyceride levels mediate the association between pre-pregnancy overweight/obesity and macrosomia among singleton term non-diabetic pregnancies: a prospective cohort study in Central China. *Nutrients* https://doi.org/10.3390/nu14102075 (2022).
40. Jeyakumar, S. M. & Vajreswari, A. Stearoyl-CoA desaturase 1: a potential target for non-alcoholic fatty liver disease?-Perspective on emerging experimental evidence. *World J. Hepatol.* **14**(1), 168–179 (2022).
41. Soldavini, C. M. et al. Gestational diabetes severity stratification during pregnancy: role of plasma oleic acid as a possible early marker. *Acta Diabetol.* **62**(9), 1549–1559 (2025).
42. Steffen, B. T., Duprez, D., Szklo, M., Guan, W. & Tsai, M. Y. Circulating oleic acid levels are related to greater risks of cardiovascular events and all-cause mortality: the multi-ethnic study of atherosclerosis. *J. Clin. Lipidol.* **12**(6), 1404–1412 (2018).
43. Sonnenschein, N. et al. A network perspective on metabolic inconsistency. *BMC Syst. Biol.* **6**, 41 (2012).
44. Dorninger, F., Forss-Petter, S., Wimmer, I. & Berger, J. Plasmalogens, platelet-activating factor and beyond—ether lipids in signaling and neurodegeneration. *Neurobiol. Dis.* **145**, 105061 (2020).
45. Aung, M. T. et al. Maternal lipidomic signatures in relation to spontaneous preterm birth and large-for-gestational age neonates. *Sci. Rep.* **11**(1), 8115 (2021).
46. Mantha, V. R., Vallejo, M. C., Ramesh, V., Jones, B. L. & Ramanathan, S. Maternal and cord serum cytokine changes with continuous and intermittent labor epidural analgesia: a randomized study. *Sci. World J.* **2012**, 607938 (2012).
47. Faltin-Traub, E. F., Boulvain, M., Faltin, D. L., Extermann, P. & Irion, O. Reliability of the Bishop score before labour induction at term. *Eur. J. Obstet. Gynecol. Reprod. Biol.* **112**(2), 178–181 (2004).
48. Mlodawski, J. et al. Repeatability and reproducibility of potential ultrasonographic Bishop score parameters. *J. Clin. Med.* https://doi.org/10.3390/jcm12134492 (2023).
49. Corwin, E. J. et al. Protocol for the Emory University African American vaginal, oral, and gut microbiome in pregnancy cohort study. *BMC Pregnancy Childbirth* **17**(1), 161 (2017).
50. To, T., Estrabillo, E., Wang, C. & Cicutto, L. Examining intra-rater and inter-rater response agreement: a medical chart abstraction study of a community-based asthma care program. *BMC Med. Res. Methodol.* **8**, 29 (2008).
51. Xiao, C. et al. Circulating short chain fatty acids and fatigue in patients with head and neck cancer: a longitudinal prospective study. *Brain Behav. Immun.* **113**, 432–443 (2023).
52. Ritchie, M. E. et al. limma powers differential expression analyses for RNA-sequencing and microarray studies. *Nucleic Acids Res.* **43**(7), e47 (2015).
53. Langfelder, P. & Horvath, S. WGCNA: An R package for weighted correlation network analysis. *BMC Bioinform.* **9**, 559 (2008).
54. Korotkevich G, Sukhov V, Sergushichev A. Fast gene set enrichment analysis. bioRxiv. 2019:060012.
55. Rohart, F., Gautier, B., Singh, A. & Ka, L. C. mixOmics: An R package for 'omics feature selection and multiple data integration. *PLoS Comput. Biol.* **13**(11), e1005752 (2017).
56. Friedman, J., Hastie, T. & Tibshirani, R. Regularization paths for generalized linear models via coordinate descent. *J. Stat. Softw.* **33**(1), 1–22 (2010).
57. Kuhn, M. Building predictive models in R using the caret package. *J. Stat. Softw.* **28**(5), 1–26 (2008).

Acknowledgements

The authors acknowledge the participants and research team of the Emory University African American Vaginal, Oral, and Gut Microbiome in Pregnancy Cohort study.

Author contributions

NSC and ALD conceived the analysis. NSC and CYC conducted dataset cleaning, transformation, and analyses with oversight from KMS, and interpreted data with assistance from ZH, XG, JA and KMS. ALD led the primary investigation in which all clinical information and biological samples were collected, with NSC collecting original data on labor duration. All authors contributed to writing and editing the manuscript, and approved the final manuscript submitted for review.

Funding

Dr. Nicole Carlson was supported by the National Institute of Nursing Research of the National Institutes of Health under Award Number K01NR016984 and R01NR019254 during research contained in this manuscript. The content is solely the responsibility of the authors and does not necessarily represent the official views of the National Institutes of Health.

Based on analysis of data from the African american vaginal, oral, and gut microbiome in Pregnancy Cohort Study (R01NR014800, R24ES029490) and the Metabolomics of Labor Dysfunction in African American Women study (K01NR016984).

Declarations

Competing interests
The authors declare no competing interests.

Ethics approval
The Emory University Institutional Review Board approved this secondary analysis, IRB #00002852, on 8/2021. All participants of this study provided informed consent for parent study participation and secondary use of their samples and data for follow-up studies. All methods carried out in this study were done so in accordance with relevant guidelines and regulations, as approved by the Emory University IRB.

Additional information
Supplementary Information The online version contains supplementary material available at https://doi.org/10.1038/s41598-026-45859-6.

Correspondence and requests for materials should be addressed to N.S.C.

Reprints and permissions information is available at www.nature.com/reprints.

Publisher's note Springer Nature remains neutral with regard to jurisdictional claims in published maps and institutional affiliations.